The vector alignments of asteroid spins by thermal torques

David Vokrouhlický[1], David Nesvorný[2] & William F. Bottke[2]

[1]*Institute of Astronomy, Charles University, V Holešovičkách 2, 180 00 Prague 8, Czech Republic*
[2]*Southwest Research Institute, 1050 Walnut St, Suite 400, Boulder, Colorado 80302, USA*

....

Collisions have been thought to be the dominant process altering asteroid rotations, but recent observations of the Koronis family of asteroids suggest that this may be incorrect. This group of asteroids was formed in a catastrophic collision several billion years ago; in the intervening period their rotational axes should have become nearly random because of subsequent collisions, with spin rates that follow a maxwellian distribution. What is seen, however, is that the observed family members with prograde spins have nearly identical periods (7.5–9.5 h) and obliquities between 42 and 50 degrees, while those with retrograde spins have obliquities between 154 and 169 degrees with periods either <5 h or >13 h. Here we show that these non-random orientations and spin rates can be explained by 'thermal torques' (arising from differential solar heating), which modify the spin states over time. In some cases, the asteroids become trapped in spin-orbit resonances. Our results suggest that thermal torques may be more important than collisions in changing the spin states (and possibly shapes) of asteroids with diameters <40 km.

Asteroid families are by-products of catastrophic disruption events (for example, ref. 1). They are identified by the clustered proper semimajor axis a, eccentricity e, and inclination I values of their members[2,3] as well as their common spectral properties[4]. Because these traits also allow us to estimate the ages of different families, family members can be used to investigate, in a constrained manner, collisional and dynamical evolution in the main belt over the last few Gyr. In contrast, non-family asteroids, which have a poorly constrained origin, are more difficult to use for this purpose.

We focus on the Koronis asteroid family, whose members are located at proper $a = 2.83$–2.95 AU, $e = 0.04$–0.09, and $\sin I = 0.032$–0.042 (ref. 5). Numerical simulations suggest that the Koronis family members were produced when an asteroid of diameter $D \simeq 60$ km struck the $D \simeq 120$ km Koronis parent body at 3 km s^{-1} (ref. 6). The approximate age of this family, based on studies of craters on asteroid (243) Ida, a member of the Koronis family observed by the Galileo spacecraft, and by collisional/dynamical evolution simulations, is 2–3 Gyr (refs 5, 7–9). Our calculations suggest that most $20 < D < 40$ km asteroids in this family have not suffered a disruption event over this time[10]. If the heavily cratered surface of (243) Ida is any guide[11], however, these asteroids have experienced numerous non-disruptive impact events since their formation.

Insights gleaned from laboratory and numerical experiments of asteroid collisions suggest that Koronis family members should have spin rates that approximately follow a maxwellian distribution and nearly random spin-axis orientations[6,12,13]. The observed rotation states of 20–40 km diameter asteroids within this family, however, are surprisingly different from these results. Led by clues that Koronis family members may have peculiar rotation rates and preferentially aligned spin vectors (which was thought to indicate that the Koronis family was young)[14,15], Slivan repeatedly observed ten Koronis family objects, including (243) Ida, for nearly a decade[16,17]. Information on these objects can be found in Table 1. Slivan found that the prograde rotators had tightly clustered values in spin period ($7.5 < P < 9.5$ h), obliquity ($42° < \epsilon < 50°$), and possibly ecliptic longitude, with the latter two implying that the spin axes of this group are truly parallel in space. We will refer to prograde objects with spin vectors near these clustered values as being in 'Slivan states'. Retrograde rotators, on the other hand, had $P < 5$ h or $P > 13$ h, $\epsilon \geq 154°$, and ecliptic longitudes that appear to span a large range of values.

Slivan's solutions have been verified in two different ways. First of all, his analysis yielded a spin vector for (243) Ida that agrees with spacecraft observations[17,18]. Second, Slivan's results have been reproduced via an independent analysis performed[17] using the methods described in refs 19 and 20. Hence, the solutions described in Table 1 appear to be robust.

Given the singular nature of the spin vectors in both the prograde and retrograde groups, we consider it extremely unlikely that collisions alone could have produced this distribution; some other explanation is needed. Here we show that the observed spin vectors are a by-product of dynamical processes that act over long time intervals. If true, these same processes should also play an important role in modifying the spin states of nearly all main belt asteroids with $D < 40$ km. Note that other than the results of refs 16 and 17, the spin states of main belt asteroids in this size range have been little explored.

Spin vector evolution model

We constructed a numerical model that tracks the evolution of an asteroid's rotation state over 4 Gyr via two processes: (1) thermal torques produced by the reflection and re-emission of sunlight from an asteroid's surface (that is, the Yarkovsky–O'Keefe–Radzievskii–Paddack effect or YORP effect)[21–23], and (2) the effect of solar

Table 1 **Spin vector information for Koronis family asteroids**

Asteroid	D (km)	P (h)	ϵ (°)	λ_1 (°)	λ_2 (°)
(311) Claudia	24	7.53	50	24	209
(534) Nassovia	34	9.47	42	55	241
(720) Bohlinia	34	8.92	50	48	236
(1223) Neckar	22	7.82	47	73	259
(158) Koronis	36	14.21	159	27	211
(167) Urda	40	13.06	163	39	225
(208) Lacrimosa	42	14.08	156	162	346
(243) Ida	28	4.63	156	–	263
(277) Elvira	28	29.69	169	51	242
(321) Florentina	28	2.87	154	94	265

Columns included mean asteroid diameter D, sidereal rotation period P, adopted mean obliquity ϵ, and two solutions for the ecliptic longitude λ, with $0° < \lambda_1 \leq 180°$ and $180° < \lambda_2 \leq 360°$ (refs 16–18). The diameter is computed from the absolute magnitude and geometric albedo estimated for each object. The uncertainty in ϵ is $\pm5°$ and the uncertainty in λ is $\pm(5°$–$20°)$. The first four asteroids rotate in a prograde sense ($\epsilon < 90°$), while the last six asteroids rotate in a retrograde sense ($\epsilon > 90°$). We also point out that an additional Koronis family asteroid, (462) Eriphyla, has recently been observed, and its size ($D = 38$ km), spin period ($P = 8.66$ h), spin-axis obliquity ($\epsilon = 57°$), and longitude ($\lambda_1 = 103°$) are all consistent with the clustered values in the prograde group (S. Slivan & M. Kaasalainen, personal communication).

 147

gravitational torques on an asteroid whose orbit changes over time due to planetary gravitational perturbations[24]. The YORP effect is related to the so-called Yarkovsky effect, a thermal radiation force that causes objects to undergo semimajor axis drift as a function of their spin, orbit, size and material properties[23]. YORP torques, although they are also dependent on these factors, are additionally affected by an object's precise shape; energy re-radiated from an irregularly shaped body (such as a propeller or windmill) allows the YORP effect to change its spin rate and obliquity over time, while energy re-radiated from a symmetrical body (such as a sphere or ellipsoid) produces no net YORP torque[21–23].

To determine how the spin-vector evolution of Koronis family members is affected by shape, we input real and artificial asteroid configurations into our model (such as the spacecraft derived shape of (243) Ida and numerous random asteroid shapes derived using numerical techniques[22,25,26]). Our results agree with previous work: the spin states of irregular shapes evolve more quickly via the YORP effect than rounded shapes and the evolutionary timescale is proportional to D^2 (refs 21–23). An example of this would be the spin-vector evolution of (243) Ida. If we input into our simulations an Ida shape model derived from Galileo spacecraft images[27], we find it evolves twice as fast as a more-rounded shape derived from lightcurve-inversion techniques[17,19,20]. Nevertheless, in each case, the spin-vector endstate reached by the test asteroid was the same;

only the timescale was different. Hence, in the runs described below, we used asteroid shapes that were realistic and which conformed to the performance expected from highly accurate shape models.

Prograde rotators captured by spin-orbit resonances

Using our model, we explored the long-term evolution of Koronis family asteroids having prograde and retrograde spins. For prograde rotators, the results relevant to the observed Koronis family members in Table 1 are those test asteroids that predominately spin down. Figure 1 shows the representative evolution of (311) Claudia, which was started with $P = 5$ h and a range of ϵ values. We find that the YORP torque affecting obliquity, defined as τ_{obl}, slowly drives ϵ toward the 0° asymptotic value and, in the process, increases $\dot{\psi}$, defined as the asteroid's precession rate with respect to the ecliptic. This occurs because $\dot{\psi} \propto \cos\epsilon/\omega$, where ω is the asteroid's rotation rate. When the initial ϵ is small, or if it becomes so in the course of the evolution, the YORP torque affecting P, defined as τ_{spin}, decelerates the rotation rate and therefore also increases the precession rate of the spin axis until the motion becomes captured in a spin-orbit resonance. In the case of the Koronis family asteroids, the first important resonance encountered is with Saturn's longitude of node (defined for low-enough inclination by $\dot{\psi} \simeq -s_6$, where s_6 is the mean frequency of Saturn's longitude of node, or $-26.34'' \, \text{y}^{-1}$; refs 28, 29). We find the capture probability is unity for ϵ smaller than $\simeq 30°$ (see also ref. 30).

Once in a spin-orbit resonance, the body's spin and resonance frame precess at the same rate, which keeps the spin-axis longitude fixed with respect to a specific value determined by the resonance while YORP torques modify the body's P and ϵ values. This explains why the prograde asteroids in Table 1 have clustered longitude values (see also Fig. 2). Note that there is a 180° ambiguity in the ecliptic longitude solutions presented in Table 1 (that is, λ_1 and λ_2).
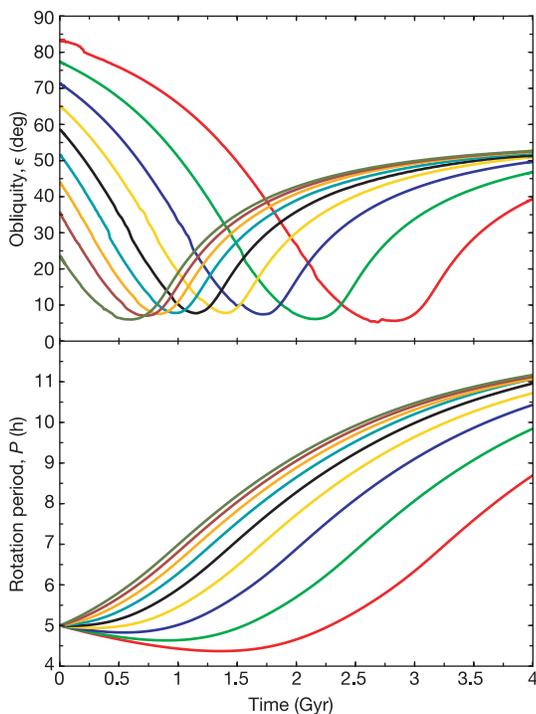
Figure 1 Several possible evolutionary paths for prograde rotator (311) Claudia, many of which evolve into Slivan states. We set Claudia's initial spin period to $P = 5$ h and its initial obliquity ϵ to uniform values in $\cos\epsilon$ between 0°–90°. We find that YORP torques modify P while driving ϵ to small values. Eventually, our test asteroids are captured by the s_6 spin-orbit secular resonance between the precession rate of the asteroid's spin axis and Saturn's longitude of node. This occurs near the minimum ϵ values for each curve shown above. Once trapped in the resonance, P steadily increases, enough to cause migration of its equilibrium (Cassini) state[30,41] and force ϵ to move toward the asymptotic value of $\simeq 55°$. We find that varying the shapes of our asteroids mainly affects the rate at which P and ϵ evolve rather than their endstate, with elongated, asymmetrical bodies evolving to the equilibrium point faster than rounded bodies. To make the figure easier to read, short-period variations in obliquity have been filtered out. Their amplitude is typically 5°–10° (especially in the resonant phase), so that all solutions, except the one starting with $\epsilon \simeq 84.3°$, are consistent with observations.
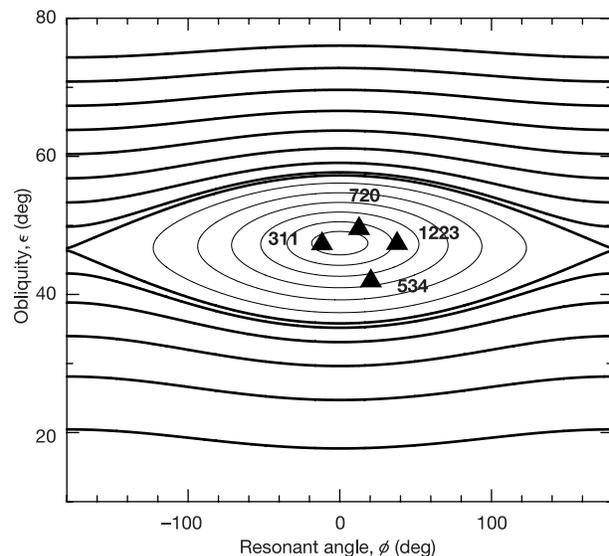
Figure 2 Prograde Koronis family members trapped in the s_6 spin-orbit resonance. This resonance is defined by $\dot{\psi} \simeq -s_6$, with $\dot{\psi}$ the precession rate and $s_6 = -26.34'' \, \text{y}^{-1}$ (the mean frequency of Saturn's longitude of node). Solid lines show the libration and circulation paths. Here we chose $\alpha/s_6 = -1.47$ and $\tau_{\text{obl}} = 0$ (see the Methods section). The abscissa is the resonant angle $\phi = -(\psi + s_6 t + \Phi_6)$, with ψ the longitude of the spin vector, t being time, and Φ_6 being the phase of the frequency term s_6. We find $\Phi_6 \simeq 307.3°$. The ordinate is the obliquity ϵ. Stable and unstable points are the Cassini states[30,41]; in this case the stable point has obliquity $\epsilon = 47°$, consistent with bodies that have evolved for 2–3 Gyr but have not yet reached their 'endstate' ($\epsilon \simeq 55°$). Symbols show projections of the prograde rotators from Table 1. Our solutions for these values use the ecliptic longitude λ_1. The prograde asteroids are located well inside the libration zone of the resonance, implying they are currently trapped in the resonance.

As we show below, our model results predict that λ_1 is the true solution. Unfortunately, ground-based observations may be unable to resolve this issue in the near future (S. Slivan, personal communication).

As τ_{spin} continues to decelerate ω, ϵ increases to maintain the resonant condition $\dot{\psi} \simeq -s_6$. Eventually, this process forces ϵ to converge to $\simeq 55°$, a value where the YORP torque τ_{spin} becomes zero for nearly all asteroid shapes[22]. At present, this surprising but important result has only been numerically determined. The $\simeq 55°$ value can probably be traced to the fact that a sphere with the same obliquity has a yearly-averaged insolation that is independent of latitude[28]. This property allows the YORP effect to drive prograde asteroids towards Slivan states (see Methods).

Depending on their shape and the particular spin-orbit resonance that produces the trapping event, asteroids in Slivan states may have a variety of P values. For example, in some of our runs, test asteroids trapped in spin-orbit resonances other than s_6 have $P > 15$ h. The prograde asteroids in Table 1, however, apparently had similar enough sizes, shapes and initial P values that all reached a Slivan states in the s_6 spin-orbit resonance after 2–3 Gyr of evolution.

We find test asteroids with initial $4 < P < 7$ h yield results similar to the Fig. 1 case. Test asteroids with $P > 7$ h, however, have initial ϵ (and $\dot{\psi}$) values that either cause them to jump or place them beyond the s_6 spin-orbit resonance. Only slow rotators started with high ϵ values have an opportunity to reach spin states like those in Table 1. The rest may eventually reach Slivan states by becoming trapped in other spin-orbit resonances, but their P values would be higher than those observed. For $P < 4$ h, we find YORP torques cannot drain rotational angular momentum out of the test asteroids fast enough for them to reach Slivan states within 4 Gyr. Thus, it is plausible that the Koronis family-forming event produced numerous $20 < D < 40$ fragments with P values originally between 4–7 h.

To check our results, we tested whether the prograde rotators were in a resonant state by projecting their observed spin vectors onto the plane of the appropriate resonant variables (Fig. 2). We find that their spin vectors cluster near the centre of the libration zone of the s_6 resonance, exactly where they should be if they are trapped in that resonance. This resonance-locking mechanism is what produces the clustered λ_1 longitude values in Table 1.

Our results indicate that (311) Claudia and (720) Bohlinia may be more elongated or asymmetrical than is suggested by their lightcurve-derived shapes[17]. We do not believe this is a problem because the methods used[17] to derive these shapes may round asteroid 'hull' dimensions by as much as 30%. Moreover, (311) Claudia exhibits lightcurve behaviour that is very similar to Ida's and cannot be fully explained by ellipsoidal models (S. Slivan, personal communication). An intriguing alternative explanation is that their spin-axis precession rates were modified over time by the presence of a kilometer-sized satellite. Note that we already know that at least one Koronis family member, (243) Ida, has a small satellite[31].

Note that all spin-orbit equilibrium points are weakly unstable and may cause asteroid spin vectors to leave the resonance after some time period (see ref. 22 for examples). This effect may have already happened to small Koronis family members (for example, $D < 10$ km), whose ϵ and P values evolve quickly via the YORP effect[21,22]. To regain a Slivan state, an asteroid needs to become trapped in another spin-orbit resonance.
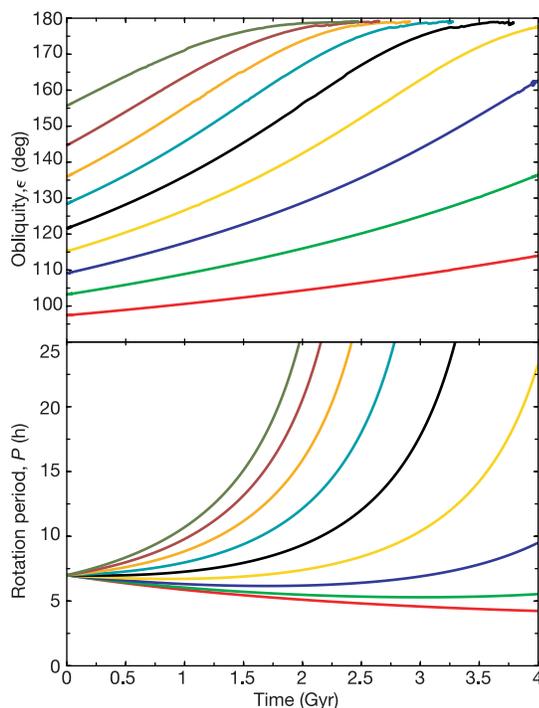
Figure 3 Several possible evolutionary paths for retrograde rotator (167) Urda, many of which evolve to slower rotation rates over 4 Gyr. We set its initial spin period to $P = 7$ h and its initial obliquity ϵ to uniform values in cos ϵ between 90°–180° (the short-period oscillations were eliminated as in Fig. 1). In most cases, YORP torques drive the obliquity ϵ towards the asymptotic value of 180° while increasing the object's rotation period P. In the remaining cases, ϵ slowly increases while P decreases. Note that there are no meaningful spin-orbit resonances for retrograde objects, so these evolutionary paths are very different from those shown in Fig. 1. The black curve provides a good match to the present state of Urda after 2–3 Gyr of evolution. The other curves provide insights into the probable evolutionary paths followed by the remaining objects in the retrograde group (Table 1).
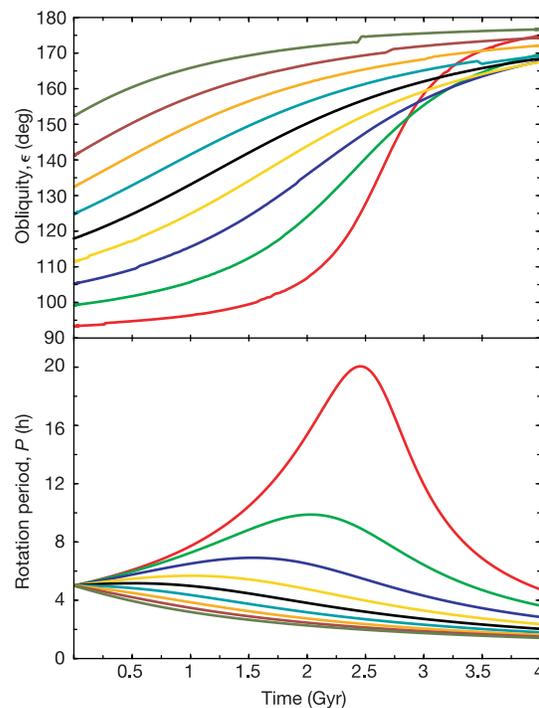
Figure 4 Several possible evolutionary paths for retrograde rotator (321) Florentina, many of which evolve to faster rotation rates. Florentina's initial spin period was set to $P = 5$ h and its initial obliquity ϵ was set uniformly in cos ϵ between 90°–180°. Like the results in Fig. 3, YORP torques drive the obliquity ϵ towards the asymptotic value of 180°. In this case, however, they decrease rather than increase the object's rotation period P. The black curve provides a good match to the present state of Florentina after 2–3 Gyr of evolution.

 149

We also investigated prograde rotators that predominately spin up rather than down. These asteroids are unlikely to be captured by the s_6 spin-orbit resonance and therefore are inconsistent with Table 1 data. For this reason, we do not discuss them further here.

Spin-vector endstates for retrograde rotators

Our model shows that retrograde rotators have their obliquity values steadily driven by the YORP effect toward the asymptotic value of $\epsilon = 180°$. By varying the initial P, ϵ values of our test asteroids, and by giving them different shapes, we found a variety of possible evolutionary paths. Some test asteroids always spin down, while others always spin up. There were even cases where objects start by spinning down but then later spin up or vice versa (Figs 3 and 4). Nevertheless, all these evolutionary paths inevitably push retrograde rotators toward the extreme P values found in Table 1.

Figure 3 shows the representative evolution of (167) Urda that was given an initial $P = 7$ h and a variety of obliquity values. We chose parameters that caused our test asteroid to predominately spin down. Because there are no important spin-orbit resonances for retrograde rotators, except for those with $P \gtrsim 60$ h, the spin states in Fig. 3 change slowly as ϵ is driven towards 180°. Gravitational planetary perturbations play a minimal role in the evolution of these objects, such that clustered longitude values are not expected. Interestingly, Table 1 shows five out of six asteroids with λ solutions within $\sim 50°$ of one another. Unlike the prograde case, however, we have no reason to think λ_1 or λ_2 is preferred.

Our results show numerous combinations of initial P, ϵ values that reproduce the spin state of (167) Urda after 2–3 Gyr of evolution. For example, depending on the ϵ value selected, initial $6 < P < 15$ h values yield reasonable matches. The only cases that do not appear to work for Urda are test asteroids with $P < 6$ h. YORP torques generally cannot eliminate enough rotational angular momentum from these bodies over 4 Gyr to match Urda's constraints.

Fast retrograde rotators like (243) Ida and (321) Florentina probably had initial shapes that forced them to predominately spin up. Figure 4 shows the representative evolution of (321) Florentina, which had observed $P = 2.87$ h. As in the Urda case, our results show many positive matches for a wide range of initial P, ϵ values. If Florentina continues along its current evolutionary path, and if it is a gravitational aggregate, it will probably shed mass in order to remove excess rotational angular momentum. Assuming that rotational disruption is analogous to tidal disruption of an asteroid/comet near a planet[32,33], this event may create a small asteroid satellite. We speculate that Dactyl, the satellite of (243) Ida, may have been produced by just such an event in the past.

Implications and predictions

We conclude that the YORP effect, working in concert with planetary perturbations, provides the most plausible means of explaining the spin rate and obliquity values of the Koronis family asteroids described in Table 1. Moreover, if the observed prograde rotators are actually trapped in the s_6 spin-orbit resonance, as indicated by our results, it would imply that collisions have played a minimal role in the evolution of ϵ and P over the last 2–3 Gyr; otherwise, we would expect that s_6 locking would have been interrupted by non-disruptive collisions. A possible explanation is that relatively little rotational angular momentum is transferred from the projectile to the target asteroid during a cratering event (for example, ref. 34).

More generally, these results suggest that, over the last several Gyr, the YORP effect may have been more efficient than collisions at changing the spin rates and obliquities of main-belt asteroids with $D < 40$ km. If true, YORP can provide a natural explanation for the plethora of $D < 40$ km asteroids with extremely fast or slow rotation rates[35]. We caution, however, that many small asteroids do not have extreme P values, implying that collisions do play some role in the evolution of their spin states. Understanding the complex interplay between collisional effects, YORP, and semimajor axis drift via the Yarkovsky effect may be critical to determining how asteroids (and meteoroids) evolve throughout the inner Solar System[36,37].

The YORP effect may also have far-reaching implications for the physical history of many small asteroids. If asteroids are predominantly gravitational aggregates (or 'rubble-pile' asteroids[38]), YORP may spin up some of them so fast that they change shape, shed mass, or even undergo fission. It may thus provide an important means of producing asteroid satellites among smaller main-belt and near-Earth asteroids (for example, timescales for spinning up kilometer-sized asteroids beyond their rotational break-up limit are a few Myr; refs 21–23).

To investigate whether asteroids in other main-belt regions may also be trapped in Slivan states, we tracked the spin-vector evolution of test prograde rotators having the same orbital parameters as (8) Flora, (15) Eunomia, (20) Massalia, (24) Themis, (37) Fides, and (221) Eos. These asteroids were chosen because they span the main belt in both semimajor axis and inclination. Our preliminary results indicate that low inclination asteroids in the outer main belt (such as (24) Themis) follow evolutionary paths similar to those described in Fig. 1; we predict that many more Slivan-state asteroids may be found there. For the rest of our test asteroids, we found more complex spin-vector evolutionary paths brought on, in part, by the presence of overlapping spin-orbit resonances. Resonance trapping events in these regions frequently force ϵ to undergo huge oscillations rather than migrating to $\simeq 55°$ (refs 22, 24, 39). Hence, to gain new insights into the history of inner main-belt asteroids or those with high inclinations, it is important first to make a careful comparison between numerical results and observations. □

Methods

Because we are interested in long-term asteroid evolution via the YORP effect, short timescales, such as the asteroid's proper rotation or its revolution around the Sun, are eliminated by averaging. The evolving parameters include the spin rate ω (rotation about the shortest axis of the inertia tensor is assumed), obliquity ϵ and precession in longitude ψ (see ref. 29 for their definition). We use the complex variable $\zeta = \sin\epsilon \exp(\iota\psi)$ to eliminate the apparent singularity at $\epsilon = 0°$ and $\epsilon = 180°$. The problem is then described by[22]:

$$\frac{d\omega}{dt} = \tau_{\text{spin}} \qquad (1)$$

$$\frac{d\zeta}{dt} = \iota\zeta(\pm\alpha\sqrt{1 - \zeta\bar{\zeta}} - 2C) \pm (\mathcal{A} - \iota\mathcal{B})\sqrt{1 - \zeta\bar{\zeta}} \mp \frac{\tau_{\text{obl}}\zeta}{\omega}\sqrt{\frac{1}{\zeta\bar{\zeta}} - 1} \qquad (2)$$

with the precession constant $\alpha = 1.5\, n^2\Delta/\omega$, n is the asteroid mean motion around the Sun, $\bar{\zeta}$ is the complex conjugate quantity, and $\Delta = 1 - (A + B)/(2C)$ with A, B and C the principal moments of the inertia tensor. Upper signs are for $0° \leq \epsilon < 90°$ and lower signs are for $90° < \epsilon \leq 180°$. We define τ_{spin} as the component of the YORP torque affecting ω and τ_{obl} the component affecting ϵ. Note that the solar torque is much more effective at determining the asteroid's precession rate than YORP. The effect of the orbital plane variations is included through the functions[29]:

$$\mathcal{A} + \iota\mathcal{B} = \frac{2}{\sqrt{1 - \xi\bar{\xi}}}\left(\frac{d\xi}{dt} - \iota\xi C\right) \qquad (3)$$

$$C = \frac{1}{2\iota}\left(\bar{\xi}\frac{d\xi}{dt} - \xi\frac{d\bar{\xi}}{dt}\right) \qquad (4)$$

where $\xi = \sin I/2 \exp(\iota\Omega)$ with the orbital inclination I and longitude of node Ω. The $\mathcal{A}$, $\mathcal{B}$, and C functions for all asteroids in our sample (Table 1) were obtained by direct numerical integration and an accurate representation with Fourier series[40]. The most important terms in this series for the Koronis family have proper and forced frequencies of $s \simeq -67''\, y^{-1}$ and $s_6 \simeq -26.34''\, y^{-1}$, respectively; the latter has a phase $\Phi_6 \simeq 307.3°$ with time origin at J2000.0.

When limited to a single periodic term, the conservative problem without YORP torques is integrable and often referred to as Colombo's top[30,41]; its equilibrium solutions are called Cassini states. In the generalized case described by equations (1) and (2), which contains the YORP effect, the equilibrium solution still exists but it now constrains obliquity to $\simeq 55°$ where $\tau_{\text{spin}} = 0$ (see text). In this case, equation (2) sets the equilibrium value of P. Performing a linear-perturbation analysis, we find that, unlike in the solely gravitational case, the equilibrium solution with YORP is unstable.

The YORP effect in equations (1) and (2) is represented by projections:

$$\tau_{\text{spin}} = \frac{\mathbf{T}\cdot\mathbf{e}}{C}, \quad \tau_{\text{obl}} = \frac{\mathbf{T}\cdot\mathbf{e}_\perp}{C} \qquad (5)$$

of the thermal torque $\mathbf{T}$ onto the spin unit vector $\mathbf{e}$ and the perpendicular vector $\mathbf{e}_\perp = [\mathbf{n} - (\mathbf{n}\cdot\mathbf{e})\mathbf{e}]/\sin\epsilon$ with $\mathbf{n}$ the unit normal to the orbital plane. Averaging over an asteroid's rotation and revolution around the Sun is assumed in equation (5). To account for shape

effects, we also average equation (5) over a large sample of gaussian random spheres[25,26] with results generalized to include the effect of finite surface conductivity (values between 0.001 to 0.01 W m^{-1} K^{-1} are used). We find that, unlike in the zero-conductivity case[22], τ_{obl} drives the ϵ value of most asteroids to the asymptotic values of 0° or 180° (see also ref. 42). When ϵ is near these values, τ_{spin} may be either positive or negative, corresponding to asymptotically decelerating or accelerating the rotation rate, respectively. For low-conductivity surfaces, the former case appears to be slightly more likely for the asteroid configurations tested.

1. Zappalà, V., Cellino, A., Dell'Oro, A. & Paolicchi, P. in *Asteroids III* (eds Bottke, W. F. *et al.*) 619–631 (Univ. Arizona Press, Tucson, 2003).

2. Knežević, Z., Lemaître, A. & Milani, A. in *Asteroids III* (eds Bottke, W. F. *et al.*) 603–612 (Univ. Arizona Press, Tucson, 2003).

3. Bendjoya, P. & Zappalà, V. in *Asteroids III* (ed. Bottke, W. F. *et al.*) 613–618 (Univ. Arizona Press, Tucson, 2003).

4. Cellino, A., Bus, S. J., Doressoundiram, A. & Lazzaro, D. in *Asteroids III* (eds Bottke, W. F. *et al.*) 632–643 (Univ. Arizona Press, Tucson, 2003).

5. Bottke, W. F., Vokrouhlický, D., Brož, M., Nesvorný, D. & Morbidelli, A. Dynamical spreading of asteroid families by the Yarkovsky effect. *Science* **294,** 1693–1696 (2001).

6. Michel, P., Benz, W., Tanga, P. & Richardson, D. C. Collisions and gravitational reaccumulation: Forming asteroid families and satellites. *Science* **294,** 1696–1700 (2001).

7. Chapman, C. R. in *Asteroids III* (eds Bottke, W. F. *et al.*) 315–329 (Univ. Arizona Press, Tucson, 2003).

8. Marzari, F., Davis, D. & Vanzani, V. Collisional evolution of asteroid families. *Icarus* **113,** 168–187 (1995).

9. Greenberg, R. *et al.* Collisional and dynamical history of Ida. *Icarus* **120,** 106–118 (1996).

10. Bottke, W. F. & Greenberg, R. in *Collisional Processes in the Solar System* (eds Marov, M. Y. & Rickman, H.) 51–71 (Kluwer Academic, Dordrecht, 2001).

11. Belton, M. J. S. *et al.* First images of asteroid 243 Ida. *Science* **265,** 1543–1547 (1994).

12. Asphaug, E. & Scheeres, D. J. Deconstructing Castalia: Evaluating a postimpact state. *Icarus* **139,** 383–386 (1999).

13. Holsapple, K., Giblin, I., Housen, K., Nakamura, A. & Ryan, E. in *Asteroids III* (eds Bottke, W. F. *et al.*) 443–462 (Univ. Arizona Press, Tucson, 2003).

14. Binzel, R. P. Collisional evolution in the Eos and Koronis asteroid families—Observational and numerical results. *Icarus* **73,** 303–313 (1988).

15. Binzel, R. P. in *Asteroids, Comets, Meteors III*, (eds Lagerkvist, C. I., Richman, H. & Lindblad, B. A.) 15–18, (Uppsala, 1990).

16. Slivan, S. M. Spin vector alignment of Koronis family asteroids. *Nature* **419,** 49–51 (2002).

17. Slivan, S. M. *et al.* Spin vectors in the Koronis family: Comprehensive results from two independent analysis of 213 rotation lightcurves. *Icarus* **162,** 285–307 (2003).

18. Davies, M. E., Colvin, T. R., Belton, M. J. S., Veverka, J. & Thomas, P. C. The direction of the north pole and the control network of asteroid 243 Ida. *Icarus* **120,** 33–37 (1996).

19. Kaasalainen, M. & Torppa, J. Optimization methods for asteroid lightcurve inversion. I. Shape determination. *Icarus* **153,** 24–36 (2001).

20. Kaasalainen, M., Torppa, J. & Muinonen, K. Optimization methods for asteroid lightcurve inversion. II. The complete inversion problem. *Icarus* **153,** 37–51 (2001).

21. Rubincam, D. P. Radiative spin-up and spin-down of small asteroids. *Icarus* **148,** 2–11 (2000).

22. Vokrouhlický, D. & Čapek, D. YORP-induced long-term evolution of the spin state of small asteroids and meteroids. Rubincam's approximation. *Icarus* **159,** 449–467 (2002).

23. Bottke, W. F., Vokrouhlický, D., Rubincam, D. P. & Brož, M. in *Asteroids III* (eds Bottke, W. F. *et al.*) 395–408 (Univ. Arizona Press, Tucson, 2003).

24. Sköglov, E., Magnusson, P. & Dahlgren, M. Evolution of the obliquities for ten asteroids. *Planet. Space Sci.* **44,** 1177–1183 (1996).

25. Muinonen, K. Introducing the Gaussian shape hypothesis for asteroids and comets. *Astron. Astrophys.* **332,** 1087–1098 (1998).

26. Muinonen, K. & Lagerros, J. S. V. Inversion of shape statistics for small solar system bodies. *Astron. Astrophys.* **333,** 753–761 (1998).

27. Thomas, P. C. *et al.* The shape of Ida. *Icarus* **120,** 20–32 (1996).

28. Ward, W. R. Climatic variations on Mars. Astronomical theory of insolation. *J. Geophys. Res.* **79,** 3375–3386 (1974).

29. Laskar, J. & Robutel, P. The chaotic obliquity of the planets. *Nature* **361,** 608–612 (1993).

30. Henrard, J. & Murigande, C. Colombo's top. *Celest. Mech.* **40,** 345–366 (1987).

31. Belton, M. J. S. *et al.* The discovery and orbit of 1993 (243)1 Dactyl. *Icarus* **120,** 185–199 (1996).

32. Richardson, D. C., Bottke, W. F. & Love, S. G. Tidal distortion and disruption of Earth-crossing asteroids. *Icarus* **134,** 47–76 (1998).

33. Asphaug, E. & Benz, W. Size, density, and structure of comet Shoemaker-Levy 9 inferred from the physics of tidal breakup. *Icarus* **121,** 225–248 (1996).

34. Love, S. G. & Ahrens, T. J. Origin of asteroid rotation rates in catastrophic impacts. *Nature* **386,** 154–156 (1997).

35. Pravec, P., Harris, A. W. & Michałowski, T. in *Asteroids III* (eds Bottke, W. F. *et al.*) 113–122 (Univ. Arizona Press, Tucson, 2003).

36. Vokrouhlický, D. & Farinella, P. Efficient delivery of meteorites to the Earth from a wide range of asteroid parent bodies. *Nature* **407,** 606–608 (2000).

37. Morbidelli, A. & Vokrouhlický, D. The Yarkovsky-driven origin of near Earth asteroids. *Icarus* **163,** 120–134 (2003).

38. Richardson, D. C., Leinhardt, Z. M., Melosh, H. J., Bottke, W. F. & Asphaug, E. in *Asteroids III* (eds Bottke, W. F. *et al.*) 501–515 (Univ. Arizona Press, Tucson, 2003).

39. Rubincam, D. P., Rowlands, D. D. & Ray, R. D. Is asteroid 951 Gaspra in a resonant obliquity state with its spin increasing due to YORP? *J. Geophys. Res.* **107**(E9), 5065 (2002).

40. Šidlichovský, M. & Nesvorný, D. Frequency modified Fourier transform and its applications to asteroids. *Celest. Mech. Dyn. Astron.* **65,** 137–148 (1997).

41. Colombo, G. Cassini's second and third laws. *Astron. J.* **71,** 891–896 (1966).

42. Čapek, D. & Vokrouhlický, D. in *'Asteroids, Comets and Meteors'* Conf. (Berlin, 2002) abstract 12-07, 117–118; at 〈http://berlinadmin.dlr.de/SGF/acm2002/〉.

Correspondence and requests for materials should be addressed to D.V. (vokrouhl@mbox.cesnet.cz).